Design of steady-state isothermal gas distribution systems consisting of long tubes in the whole range of the Knudsen number

Serafeim Misdanitis and Dimitris Valougeorgis[a)]
Department of Mechanical Engineering, University of Thessaly, Leoforos Athinon Pedion Areos, 38834 Volos, Greece

(Received 24 May 2011; accepted 7 September 2011; published 5 October 2011)

A novel algorithm is developed to solve steady-state isothermal vacuum gas dynamics flows through pipe networks consisting of long tubes based on linear kinetic theory. For a pipe network of known geometry the algorithm is capable of computing the mass flow rates (or the conductance) through the pipes as well as the pressure heads at the nodes of the network. The pressure distribution along each pipe element may also be found. Since a linear kinetic approach is implemented the analysis is valid and the results are accurate in the whole range of the Knudsen number, provided that the local pressure gradient along each tube of the network is small. This latter condition is satisfied when the channel is sufficiently long. The involved computational effort is very small. This is achieved by successfully integrating the linear kinetic results for the single tubes into the general solver for designing the gas pipe network. To demonstrate the feasibility of the approach two typical piping systems one in the range of small and a second one in the range of moderate Knudsen numbers are simulated. The proposed algorithm simulates, in an exact manner, low-speed gas distribution systems under any vacuum conditions based on linear kinetic modeling and constitutes a significant advancement tool in vacuum technology. © *2011 American Vacuum Society*. [DOI: 10.1116/1.3645582]

I. INTRODUCTION

Steady-state isothermal rarefied gas flows in long circular channels have been extensively investigated via linear kinetic theory from the 1960s, implementing various semianalytical and numerical schemes. An extended and profound review is given by Sharipov.[1] Also, internal gas flows in channels of various cross sections (orthogonal, ellipsoidal, circular annulus, triangular) under any degree of gas rarefaction has been studied by the integro-moment method[2,3] and more recently by the discrete velocity method.[4–7] It is noted that linear kinetic modeling is applicable, when the local pressure gradient along the tube is small. This condition is satisfied in the case of long tubes (e.g. the ratio of the length over the radius to be approximately larger than 100), resulting to a low speed isothermal flow even if the overall difference between the inlet and outlet pressure is large.[8] In addition, in the case of long channels the end effects, i.e., losses in the inlet and outlet sections and connections of the tube, are small compared to the losses through the tube and may be neglected. Beaming effects are also not significant when the channel is sufficiently long. These arguments are supported by the very good agreement obtained between kinetic and corresponding experimental results measured in advanced vacuum and micro experimental facilities.[9,10] Overall it has been demonstrated that for rarefied gas flows in long channels, linear kinetic modeling, as described by suitable kinetic model equations, may take advantage of all flow characteristics and properties and yield very accurate results in the whole range of the Knudsen number with minimal computational effort.

In many applications, however, the rarefied gaseous distribution system consists not only of a single channel but of many channels accordingly combined to form a network. Such distribution systems are commonly found in several technological fields including vacuum pumping, metrology, industrial aerosol, porous media, and microfluidics. It is pointed out that computational algorithms dedicated to the design of gas pipe networks (e.g., compressed air, natural gas, etc.) in the viscous regime are well developed,[11–13] while corresponding tools for the design of gaseous pipe networks operating under any (e.g. low, medium, and high) vacuum conditions are very limited.

In the free molecular limit a vacuum system consisting of many elements has been simulated by converting it first into a vacuum circuit network and then to an analogous electric circuit.[14,15] This concept is valid when the whole system is under very high vacuum conditions and intermolecular collisions are negligible. As far as the authors are aware of, simulations of complex gas distribution systems in the transition regime have been performed only by the ITERVAC[16] code. This code has been developed within the European fusion program in an effort to simulate the primary vacuum system of the tokamak-type fusion reactor ITER, which is under construction in south France. ITERVAC is an advanced computational tool for the simulation of the mass flow through ducts at isothermal conditions in a wide flow regime. However, it is subject to certain theoretical simplifications, while the implemented expressions, for estimating the conductance through various pipe elements, are empirical based on interpolation between free molecular and viscous results.

In the present work a computational approach based on solid theoretical principals is presented for the design of steady-state isothermal pipe networks consisting of long tubes in the whole range of the Knudsen number. This is

[a)]Electronic mail: diva@mie.uth.gr

achieved by successfully integrating the linear kinetic results obtained for the rarefied flow through each tube of the network into a typical network algorithm solving the whole distribution system. Once the geometry of the network is fixed, the integrated algorithm may successfully handle gas pipe networks consisting of long tubes of any complexity operating under any rarefied conditions from the free molecular, through the transition up to the slip and hydrodynamic regimes. It is emphasized that the range of applicability of the proposed algorithm is the same with the range of applicability of solving low-speed isothermal rarefied gas flows through long channels based on linear kinetic theory.[1–8]

II. FORMULATION

A typical pipe network may be considered as a directed linear graph consisting of a finite number of pipe sections interconnected in a specified configuration. Each pipe is characterized of its length L, diameter D and some roughness. A point where two or more pipes are joined is known as a junction node or simply as a node. The closed path uniquely formed by adjacent pipes is a loop, while the open path connecting two fixed-grade nodes is a pseudoloop. A fixed grade node is a node where a consistent energy grade is maintained (e.g. a constant pressure reservoir). For a well-defined network with p pipes, n junction nodes, l loops, and f fixed-grade nodes the following relation holds:[13]

$$p = n + l + f - 1. \tag{1}$$

Usually the geometry of the network is specified and the objective is to compute the flow quantities, i.e., the mass flow rate (or the conductance) through each tube and the pressure head at each node.

Independent of the flow regime, the system of equations describing such a network consists of the pressure drop equations along each pipe element and the mass conservation equations at each node of the network. The pressure drop equations may be reduced to a set of the energy balance equations for the closed loops of the network, which along with the mass conservation equations form a closed set to be solved for the unknown mass flow rates. Then, the pressure heads at the nodes are estimated through the pressure drop equations. When the Knudsen number characterizing the flow through the network is very small and the flow is in the continuum (or viscous) or slip regimes, then the pressure drop equations along each channel are given by closed form algebraic expressions and their integration in the whole algorithm is straightforward. In contrary, when the flow is in the transition regime such expressions are not available. This is a serious pitfall which may be circumvented if the pressure drop will be provided by solving these channel flows under any vacuum conditions. Here, this information is obtained from a data base, which has been developed for this purpose by solving a linearized kinetic equation in the whole range of the Knudsen number and obtaining the corresponding data.

Based on the above, in Sec II. A all necessary information of the kinetic solution for rarefied flow through a single tube is provided, while in Sec. II. B the integrated algorithm for the flow solution of the whole network is described.

A. Single pipe formulation

The solution of a pressure driven isothermal rarefied gas flow through a long circular tube based on linear kinetic theory is a very well known problem[1] and therefore here, only information which is directly connected and needed to the solution of the whole network is reviewed. Since $D \ll L$, the flow is considered as fully developed and therefore the pressure (or density) varies only in the flow direction being constant at each cross section, while end effects at the connecting nodes of the channel as well as beaming effects are ignored.

The mass flow rate at each cross section through the tube is given by[1,7–9]

$$\dot{M} = 2\pi \int_0^{D/2} \rho(\tilde{z})\tilde{u}(\tilde{r})\tilde{r}d\tilde{r}, \tag{2}$$

where $0 \le \tilde{r} \le D/2$ is the radial direction, $0 \le \tilde{z} \le L$ is the flow direction, $\rho(\tilde{z})$ is the mass density and $\tilde{u}$ $(\tilde{r})$ is the bulk velocity. Also, the equation of state is given by $\rho = 2P/\upsilon_0^2$, where $P = P(\tilde{z})$ is the local pressure along the tube and $\upsilon_0 = \sqrt{2RT_0}$, with R denoting the gas constant and T_0 a reference temperature, is the most probable molecular velocity. The diameter D and the molecular velocity υ_0 are taken as the characteristic length and velocity, respectively. By substituting into Eq. (2) the equation of state, as well as the dimensionless variables $\mathrm{r} = \tilde{r}/D$, $z = \tilde{z}/D$, $\mathrm{u} = \tilde{u}/(\upsilon_0 X_P)$ with $X_P = (D/P)(dP/d\tilde{z})$ denoting the local pressure gradient, yields

$$\dot{M} = G(\delta)\frac{\pi D^3}{4\upsilon_0}\frac{dP}{d\tilde{z}}. \tag{3}$$

The quantity $G(\delta) = 16\int_0^{1/2} u(r)rdr$ is the local dimensionless flow rate, which depends on the local rarefaction parameter δ, and it is obtained by solving a suitably chosen linearized kinetic model equation subject to some boundary condition. Tabulated results of $G(\delta)$ may be found in Ref. 9 (Table IV) in the whole range of δ. Also, in the hydrodynamic regime, i.e., as $\delta \to \infty$, $G(\delta) = \delta/16$. The local rarefaction parameter δ is defined as

$$\delta = \frac{PD}{\mu\upsilon_0} = \frac{\sqrt{\pi}}{2}\frac{1}{\mathrm{Kn}}, \tag{4}$$

with μ denoting the gas viscosity at reference temperature T_0 and it is in general proportional to the inverse Knudsen number. The specific relation between δ and Kn, as specified in Eq. (4), is valid in the case of hard sphere molecules.

Following a straightforward procedure,[1,8,9,17] it is found that

$$\dot{M} = G^*\frac{\pi D^3}{4\upsilon_0}\frac{P_1 - P_2}{L}, \tag{5}$$

where P_1 and P_2 denote the pressure at the two ends of the tube and

$$G^* = \frac{1}{\delta_1 - \delta_2}, \int_{\delta_1}^{\delta_2} G(\delta) d\delta. \tag{6}$$

The values δ_1, δ_2 correspond to P_1, P_2 and denote the rarefaction parameters at the two ends of the tube. The average Knudsen number of the flow is defined as

$$\mathrm{Kn}_{\mathrm{ave}} = \frac{2}{\sqrt{\pi}} \left(\frac{1}{\delta_{\mathrm{ave}}} \right) = \frac{2}{\sqrt{\pi}} \left(\frac{2}{\delta_1 + \delta_2} \right). \tag{7}$$

Once the mass flow rate is found the conductance C is easily computed as[18]

$$C = \frac{\dot{M}}{m} \frac{RT_0}{(P_1 - P_2)} \tag{8}$$

with m denoting the molar mass of the gas. Also, the pressure distribution along the tube may be computed by rearranging Eq. (3) and solving the resulting ordinary differential equation[1,8,9,17] for the unknown $P = P(z)$.

For the purposes of the present work, the dimensionless flow rates are estimated based on the linearized BGK equation with diffuse boundary conditions. Results of the quantity G(δ) are obtained from Ref. 9 or if additional estimates in terms of δ, not provided in Ref. 9 are needed, they are computed. These results are kept in a data base and are used in the solution of the network. In particular, in the process of solving the whole network the pressures P_1, P_2 and therefore δ_1, δ_2 are estimated and then the values of, $G(\delta)$ obtained from the data base are used in the integration according to Eq. (6) to yield G^*, which is substituted next into Eq. (5) to deduce the mass flow rate for each pipe section of the network.

B. Generalized network equations

As mentioned above the initial system of equations describing the network consists of the pressure drop equations along each piping element and the mass conservation equations at each node of the network. The pressure drop equations are given by solving Eq. (5) for the pressure difference to yield

$$(P_1 - P_2)_j = \Delta P_j = 4 \frac{\dot{M}_j}{G_j^*} \frac{L_j \upsilon_0}{\pi D_j^3}, \tag{9}$$

where the index $1 \le j \le p$ denotes each of the p pipes of the network. The mass conservation equations may be expressed as[13]

$$\left[\sum_j (\pm) \dot{M}_j - Q \right]_i = 0, \tag{10}$$

where the index $1 \le i \le n$ denotes each of the n junction nodes of the network, while the summation index j refers to the pipes connected to the node i, while $Q = Q_i$ is the external demand (if any) at node i. The plus and minus signs are used for flow into and out of the node i respectively. Equations (9) and (10) are coupled and may be solved for the unknown pressure heads and mass flow rates.

However, it is convenient to reduce the number of equations by combining the pressure drop Eq. (9) along each uniquely determined closed loop of the network to derive the so-called energy balance equations given by[13]

$$\left[\sum_j (\pm)(\Delta P_j) \right]_k = 0. \tag{11}$$

Here the summation index j pertains to the pipes that make up a loop, while the index $1 \le k \le l$, denotes each of the l loops. The plus sign is used if the flow in the element is positive in the clockwise sense; otherwise the minus sign is employed. By substituting Eq. (9) into Eq. (11), the energy balance equations become

$$\left[\sum_j (\pm) \left(4 \frac{\dot{M}_j}{G_j^*} \frac{L_j \upsilon_0}{\pi D_j^3} \right) \right]_k = 0. \tag{12}$$

Following this procedure, the pressure heads have been eliminated and Eqs. (10) and (12) form a well defined system having as unknowns only the mass flow rates $\dot{M}_j$. Once this system is solved for the mass flow rates then, the pressure heads are obtained from Eq. (9). When there are fixed-grade nodes in the network then, the system of equations for the mass flow rates is amplified by the energy balance equation around each pseudoloop connecting two fixed grade nodes according to

$$\left[\sum_j (\pm) \left(4 \frac{\dot{M}_j}{G_j^*} \frac{L_j \upsilon_0}{\pi D_j^3} \right) + \Delta H \right]_m = 0. \tag{13}$$

Here, the summation index j pertains to the pipes that make up a pseudoloop, the index $1 \le m \le f - 1$, denotes each of the $f - 1$ pseudoloops (f is the number of fixed grade nodes) and ΔH is the difference in magnitude of the fixed-grade nodes in the path ordered in a clockwise fashion across the imaginary pipe in the pseudoloop. The plus and minus signs follow the same arguments given for Eqs. (11) and (12).

Based on the above the final system of equations will consist of $n + l + f - 1$ equations to be solved for the p unknown mass flow rates $\dot{M}_j$. This clearly explains why for a well defined pipe network relation (1) must be satisfied. However, it is important to note that since in the system consisting of Eqs. (10), (12), and (13) the quantities G_j^* are not known *a priori*, an overall iterative algorithm incorporating Eq. (9) is needed. The detailed description of this algorithm is presented in the next section.

III. NUMERICAL ALGORITHM

The developed code includes first the drawing of the network in a graphical environment and then the formulation and solution of the governing equations describing the flow

conditions of the distribution system. The code is capable of providing the input data and solving pipe networks of any complexity.

The drawing of the network and the input of the data are prepared on a graphical user interface (GUI). The development of the graphic interface is based on available GNU General Public License (GPL) libraries including some new libraries written in javascript to match the needs of the application. As a result, the user is able to draw the desired network by adding nodes and pipe sections and the corresponding data, i.e., the coordinates of the nodes in a 3D space, the length and the diameter of the pipe elements, the pressure heads of the fixed-grade nodes and information for the type of the gas and its properties (viscosity, most probable molecular velocity, etc.). The demands (if any) at the nodes are also provided. Therefore, a connectivity matrix for each node and tube of the network is formed providing all necessary information as input data. In addition, the code is scanning to find all possible closed loops, keeping finally only the l uniquely determined loops consisting of the least number of piping elements and the $f-1$ pseudoloops between the f fixed-grade nodes.

Once the network is drawn, the resulting input file is introduced into a Fortran code. The code is based on an iterative process between the pressure drop Eq. (9) and the system of mass and energy conservation equations consisting of Eqs. (10), (12), and (13), which may be summarized as follows:

1. At all nodes of the network, where the pressure is unknown it is initially assumed and the pressure differences ΔP_j along each tube $1 \le j \le p$ are stored.
2. The rarefaction parameter at each node is estimated by Eq. (4).
3. The quantity G_j^*, $1 \le j \le p$, is estimated by Eq. (6) for each tube using the available data base for the dimensionless flow rate G (δ). Cubic splines are used to interpolate if needed between the values provided in the data base.
4. The system of mass conservation and energy balance Eqs. (10), (12), and (13) is solved by applying Gauss elimination with full pivoting to compute the mass flow rates $\dot{M}_j$ through each tube $1 \le j \le p$.
5. Equation (9) is solved to estimate the updated pressure drops ΔP_j.
6. The updated values of ΔP_j are compared with the ones in step 1, and the whole process is repeated upon convergence.

It is noted that the iterative process will converge under any initial conditions provided that all data characterizing the loops and pseudoloops of the network, including Eq. (1), are properly given. A detailed flow diagram of the developed algorithm is shown in Fig. 1.

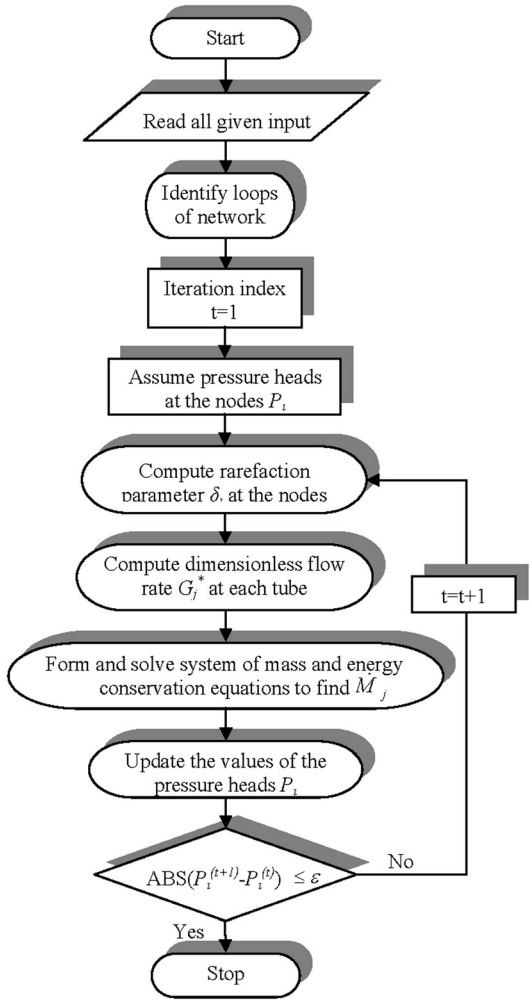

FIG. 1. Flow diagram of the algorithm.

IV. RESULTS AND DISCUSSION

To demonstrate the feasibility and the effectiveness of the proposed methodology the sample network shown in Fig. 2 is simulated. The network consists of $p=42$ tubes $n=25$ junction nodes {2,3,..,25,26}, $f=2$ fixed-grade nodes {1,27} and $l=16$ loops ($p=n+l+f-1$). Nodes 1 and 27 refer to two reservoirs, where the pressure is held constant. All tubes are taken to have the same length and diameter, which are equal to $L=10$ m and $D=0.1$ m, respectively. The reference temperature is set to $T_0=290.68$ K. The conveying gas is nitrogen (N_2), with molar mass $m=0.0280314$ kg/mol, gas constant $R=296.92$ J/(kg · K), most probable molecular velocity $v_0=415.47$ m/s and viscosity $\mu=1.73562(-5)$ Pa · s.

Then, the system of governing equations includes 25 mass conservation equations at the junction nodes, 16 energy balance equations for the closed loops, and 1 energy balance equation for the open pseudoloop formed along the nodes {1,2,3,4,5,6,11,16,21,26,27}. The total number of equations of the system is 42 and its solution returns the 42 unknown mass flow rates $\{\dot{M}_1, \dot{M}_2, ..., \dot{M}_{42}\}$ and the corresponding conductances $\{C_1, C_2, .., C_{42}\}$. Then, from the pressure drop equations the pressure heads $\{P_2, .., P_{26}\}$ are found. Finally, the pressure distribution along each pipe element of the network may also be estimated based on Eq. (3).

Two typical simulations are performed the first one in the viscous (or hydrodynamic) regime (Sec. IV. A) and the second one in a wide range of the Knudsen number (Sec. IV. B). The former is used to benchmark and validate the algorithm

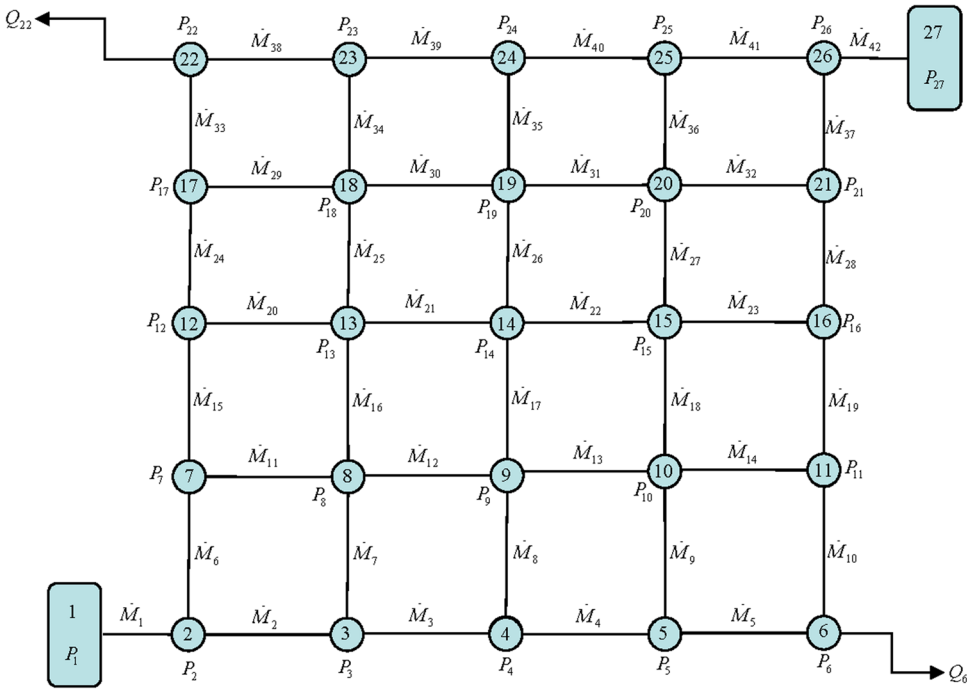

FIG. 2. (Color online) Sample network configuration.

and the results and the latter one to demonstrate the applicability of the whole approach in all flow regimes. This is easily adjusted by accordingly varying at the two fixed-grade nodes the pressures P_1 and P_{27}.

A. Algorithm validation in the viscous regime

The pressure at nodes 1 and 27 is set equal $P_1 = 70\,\text{Pa}$ and $P_{27} = 60\,\text{Pa}$. The corresponding Knudsen numbers are 9.13×10^{-4} and 1.07×10^{-3}, which clearly indicates that the flow in the network is in the viscous (or hydrodynamic) regime. For generality purposes, demands (or leakages) have been added at nodes 6 and 22, which are equal to $Q_6 = 1.40 \times 10^{-5}\,\text{kg/s}$ and $Q_{22} = 2.10 \times 10^{-5}\,\text{kg/s}$, respectively.

In Table I, the computed Knudsen number and pressure at each node of the network are tabulated, while in Table II, the mass flow rate and the conductance along each tube of the network are presented. The negative values at some of the mass flow rates indicate that the final direction of the flow in this tube is opposite to the one initially assumed. The total mass flow in tube 1 is $4.33 \times 10^{-5}\,\text{kg/s}$, while in tube 42 is $8.32 \times 10^{-6}\,\text{kg/s}$. The difference between these two quantities is $3.50 \times 10^{-5}\,\text{kg/s}$, which is equal to the total demand in nodes 6 and 22, i.e., as expected $\dot{M}_1 = \dot{M}_{42} + Q_6 + Q_{22}$.

To benchmark the present formulation and results this network subject to exactly the same conditions has been also solved using a typical hydrodynamic solver for gas pipe networks and a comparison between the results is performed. A gaseous pipe network in the viscous (or hydrodynamic) regime is still described by Eqs. (10), (12), and (13) and the only difference compared to networks operating under rarefied conditions is that the pressure drop along each pipe element, instead of Eq. (9) which is based on kinetic theory, is obtained by a corresponding expression based on hydrodynamic principals. For the purposes of the present work the Darcy–Weisbach equation is implemented:

$$(P_1 - P_2)_j = \Delta P_j = 8 \frac{\dot{M}_j^2}{\rho_j \pi^2 D_j^4} \left(2 \ln \frac{P_1}{P_2} + f_j \frac{L_j}{D_j} \right). \tag{14}$$

Here, the index $1 \le j \le p$ denotes again each of the p pipes of the network, ρ_j is the average value of the mass density and f_j. is the friction factor. In the present case the flow is laminar and $f_j = 64/\text{Re}_j$, where Re_j is the average Reynolds number at the jth pipe. The agreement between the results based on the hydrodynamic analysis and the ones based in kinetic theory, shown in Tables I and II, is excellent. In

TABLE I. Pressure and Knudsen number at each node of the network in the viscous regime.

Node number	Kn	Pressure [Pa]	Node number	Kn	Pressure [Pa]
1	9.13×10^{-4}	70.00	15	1.03×10^{-3}	61.77
2	9.66×10^{-4}	66.12	16	1.04×10^{-3}	61.52
3	9.97×10^{-4}	64.13	17	1.04×10^{-3}	61.58
4	1.02×10^{-3}	62.90	18	1.04×10^{-3}	61.71
5	1.03×10^{-3}	61.98	19	1.04×10^{-3}	61.66
6	1.05×10^{-3}	61.05	20	1.04×10^{-3}	61.49
7	9.97×10^{-4}	64.07	21	1.04×10^{-3}	61.28
8	1.01×10^{-3}	63.32	22	1.06×10^{-3}	60.30
9	1.02×10^{-3}	62.58	23	1.05×10^{-3}	61.12
10	1.03×10^{-3}	61.96	24	1.04×10^{-3}	61.34
11	1.04×10^{-3}	61.51	25	1.04×10^{-3}	61.22
12	1.02×10^{-3}	62.72	26	1.05×10^{-3}	60.84
13	1.02×10^{-3}	62.47	27	1.07×10^{-3}	60.00
14	1.03×10^{-3}	62.12			

TABLE II. Mass flow rate and conductance at each tube of the network in the viscous regime.

Tube number	From node to node	$\dot{M}_j$ [kg/s]	C_j [lt/s]	Tube number	From node to node	$\dot{M}_j$ [kg/s]	C_j [lt/s]
1	1–2	4.33×10^{-5}	9.06×10^{2}	22	15–14	-3.55×10^{-6}	8.25×10^{2}
2	2–3	2.13×10^{-5}	8.67×10^{2}	23	16–15	-2.54×10^{-6}	8.21×10^{2}
3	3–4	1.28×10^{-5}	8.46×10^{2}	24	17–12	-1.16×10^{-5}	8.28×10^{2}
4	4–5	9.49×10^{-6}	8.32×10^{2}	25	18–13	-7.74×10^{-6}	8.27×10^{2}
5	5–6	9.35×10^{-6}	8.20×10^{2}	26	19–14	-4.66×10^{-6}	8.25×10^{2}
6	7–2	-2.20×10^{-5}	8.67×10^{2}	27	15–20	2.92×10^{-6}	8.21×10^{2}
7	3–8	8.52×10^{-6}	8.49×10^{2}	28	16–21	2.43×10^{-6}	8.18×10^{2}
8	9–4	-3.33×10^{-6}	8.36×10^{2}	29	17–18	-1.29×10^{-6}	8.21×10^{2}
9	10–5	-1.47×10^{-7}	8.26×10^{2}	30	19–18	-4.75×10^{-7}	8.22×10^{2}
10	6–11	-4.65×10^{-6}	8.17×10^{2}	31	20–17	-1.81×10^{-6}	8.20×10^{2}
11	7–8	7.88×10^{-6}	8.48×10^{2}	32	20–21	2.05×10^{-6}	8.18×10^{2}
12	8–9	7.64×10^{-6}	8.38×10^{2}	33	22–17	-1.28×10^{-5}	8.12×10^{2}
13	10–9	-6.31×10^{-6}	8.30×10^{2}	34	23–18	-5.98×10^{-6}	8.18×10^{2}
14	11–10	-4.55×10^{-6}	8.23×10^{2}	35	24–19	-3.33×10^{-6}	8.19×10^{2}
15	12–7	-1.41×10^{-5}	8.44×10^{2}	36	25–20	-2.68×10^{-6}	8.17×10^{2}
16	8–13	8.76×10^{-6}	8.38×10^{2}	37	21–26	4.48×10^{-6}	8.14×10^{2}
17	9–14	4.66×10^{-6}	8.31×10^{2}	38	23–22	8.15×10^{-6}	8.09×10^{2}
18	10–15	1.91×10^{-6}	8.24×10^{2}	39	24–23	2.17×10^{-6}	8.16×10^{2}
19	11–16	-1.04×10^{-7}	8.20×10^{2}	40	25–24	-1.16×10^{-6}	8.16×10^{2}
20	12–13	2.54×10^{-6}	8.34×10^{2}	41	26–25	-3.84×10^{-6}	8.13×10^{2}
21	13–14	3.55×10^{-6}	8.30×10^{2}	42	26–27	8.32×10^{-6}	8.05×10^{2}

particular, the corresponding results of pressure at each node and mass flow rate in each tube, agree up to at least two significant figures. Therefore, the hydrodynamic results are not shown here. This result provides additional confidence in the accuracy of the developed gas pipe algorithm based on linear kinetic theory for simulating steady-state low-speed gas piping networks consisting of long tubes.

B. Results in a wide range of the Knudsen number

In this simulation the pressure at nodes 1 and 27 is set equal $P_1 = 1$ Pa and $P_{27} = 0.001$ Pa, respectively, while the corresponding Knudsen numbers are 0.0639 and 63.9, which clearly indicates that the flow in the network covers the slip, transition, and free molecular regimes. Also, the demands at all nodes have been set equal to zero. The results of the simulation include the computed Knudsen number and pressure at each node of the network in Table III, as well as the mass flow rate and the conductance along each tube of the network in Table IV. Again, the negative values at some of the mass flow rates indicate that the final direction of the flow in this tube is opposite to the one initially assumed. The total mass flow rate which is transferred from node 1 through the network to node 27 is equal to 4.58×10^{-8} kg/s and since there are no demands or leakages in the network $\dot{M}_1 = \dot{M}_{42}$. The corresponding conductances are $C_1 = 20.4$ lt/s and $C_{42} = 11.4$ lt/s. As expected the network solution, due to the specific geometry and data, is symmetric about an axis defined by nodes {2,8,14,20,26}.

The present network setup has been also simulated by implementing the typical hydrodynamic solver resulting to significant discrepancies compared to the corresponding kinetic results throughout the network (pressure heads off by about 40% and total mass flow rate off by about 100%). It is interesting to note that although most of the nodes are in the slip regime with only one node (Node 27) in the free molecular regime the viscous analysis is not applicable.

In order to provide an estimation of the involved computational effort it is noted that the solution of this sample network requires the CPU time of about 2 s on a 3 Ghz dual core system. It is obvious that the involved computational effort is negligible. For more complex networks consisting of hundreds of tubes the computational effort will be increased but not significantly. Since the data base of the kinetic results is available the computational effort is related only to the number of iterations needed for the convergence

TABLE III. Pressure and Knudsen number at each node of the network in all regimes.

Node number	Kn	Pressure [Pa]	Node number	Kn	Pressure [Pa]
1	6.39×10^{-2}	1.00	15	1.14×10^{-1}	5.59×10^{-1}
2	7.81×10^{-2}	8.18×10^{-1}	16	1.20×10^{-1}	5.33×10^{-1}
3	8.90×10^{-2}	7.18×10^{-1}	17	1.04×10^{-1}	6.16×10^{-1}
4	9.74×10^{-2}	6.56×10^{-1}	18	1.07×10^{-1}	5.96×10^{-1}
5	1.04×10^{-1}	6.16×10^{-1}	19	1.14×10^{-1}	5.59×10^{-1}
6	1.07×10^{-1}	5.96×10^{-1}	20	1.25×10^{-1}	5.11×10^{-1}
7	8.90×10^{-2}	7.18×10^{-1}	21	1.39×10^{-1}	4.60×10^{-1}
8	9.46×10^{-2}	6.75×10^{-1}	22	1.07×10^{-1}	5.96×10^{-1}
9	1.01×10^{-1}	6.31×10^{-1}	23	1.11×10^{-1}	5.75×10^{-1}
10	1.07×10^{-1}	5.96×10^{-1}	24	1.20×10^{-1}	5.33×10^{-1}
11	1.11×10^{-1}	5.75×10^{-1}	25	1.39×10^{-1}	4.60×10^{-1}
12	9.74×10^{-2}	6.56×10^{-1}	26	1.95×10^{-1}	3.27×10^{-1}
13	1.01×10^{-1}	6.31×10^{-1}	27	6.39×10^{1}	1.00×10^{-3}
14	1.07×10^{-1}	5.96×10^{-1}			

TABLE IV. Mass flow rate and conductance at each tube of the network in all regimes.

Tube number	From node to node	$\dot{M}_j$ [kg/s]	C_j [lt/s]	Tube number	From node to node	$\dot{M}_j$ [kg/s]	C_j [lt/s]
1	1–2	4.58×10^{-8}	20.4	22	15–14	-7.28×10^{-9}	16.2
2	2–3	2.29×10^{-8}	18.6	23	16–15	-5.20×10^{-9}	15.8
3	3–4	1.35×10^{-8}	17.6	24	17–12	-8.32×10^{-9}	16.9
4	4–5	8.32×10^{-9}	16.9	25	18–13	-7.28×10^{-9}	16.6
5	5–6	4.16×10^{-9}	16.5	26	19–14	-7.28×10^{-9}	16.2
6	7–2	-2.29×10^{-8}	18.6	27	15–20	9.36×10^{-9}	15.7
7	3–8	9.36×10^{-9}	17.7	28	16–21	1.35×10^{-8}	15.2
8	9–4	-5.20×10^{-9}	17.0	29	17–18	4.16×10^{-9}	16.5
9	10–5	-4.16×10^{-9}	16.5	30	19–18	-7.28×10^{-9}	16.2
10	6–11	4.16×10^{-9}	16.3	31	20–17	-9.36×10^{-9}	15.6
11	7–8	9.36×10^{-9}	17.7	32	20–21	9.36×10^{-9}	15.0
12	8–9	9.36×10^{-9}	17.1	33	22–17	-4.16×10^{-9}	16.5
13	10–9	-7.28×10^{-9}	16.6	34	23–18	-4.16×10^{-9}	16.3
14	11–10	-4.16×10^{-9}	16.3	35	24–19	-5.20×10^{-9}	15.8
15	12–7	-1.35×10^{-8}	17.6	36	25–20	-9.36×10^{-9}	15.0
16	8–13	9.36×10^{-9}	17.1	37	21–26	2.29×10^{-8}	13.9
17	9–14	7.28×10^{-9}	16.6	38	23–22	-4.16×10^{-9}	16.3
18	10–15	7.28×10^{-9}	16.2	39	24–23	-8.32×10^{-9}	15.9
19	11–16	8.32×10^{-9}	15.9	40	25–24	-1.35×10^{-8}	15.2
20	12–13	5.20×10^{-9}	17.0	41	26–25	-2.29×10^{-8}	13.9
21	13–14	7.28×10^{-9}	16.6	42	26–27	4.58×10^{-8}	11.4

of the iteration scheme and the solution of the algebraic system in each iteration.

V. CONCLUDING REMARKS

A novel algorithm has been developed for the design of steady-state, isothermal gaseous distribution systems consisting of long tubes based on linear kinetic theory. The drawing of the network is aided by a GUI interface, the output of which is directly linked to the main iterative algorithm for designing gas pipe networks. More important the main algorithm successfully integrates linear kinetic results available from a data base. The kinetic results have been obtained by solving the linearized BGK equation with diffuse boundary conditions in the whole range of the Knudsen number. As a result the integrated algorithm may successfully handle gas pipe networks consisting of long tubes of any complexity operating under any vacuum conditions from the free molecular, through the transition up to the slip and hydrodynamic regimes yielding the mass flow rate (and the conductance) through the pipes as well as the pressure and the Knudsen number at the nodes of the network. The effectiveness of the methodology has been demonstrated by solving a network of moderate complexity (1) in the viscous regime and (2) in the whole range of the Knudsen number in a very computationally efficient manner. The developed algorithm may be easily extended to include channels of any cross section.

It is noted that in the present analysis the pressure losses in the inlet and outlet connections of each tube as well as end and beaming effects have been considered as significantly smaller than the pressure losses through the pipes and have not been included in the algorithm. These assumptions are justified by the fact that the network consists of sufficiently long channels and the flow is low-speed and isothermal. The extension of the algorithm to pipe networks consisting not only of long channels but also of channels of finite length including piping elements such as bends and tees is important and challenging. This extension of the code will be reachable once the available kinetic data base is enhanced with the corresponding results based on nonlinear kinetic analysis.

It is hoped that the present work will constitute a significant part of a more general algorithm which will be used as a significant engineering tool in the design and optimization of gaseous distribution networks operating under any rarefied conditions.

ACKNOWLEDGMENTS

This work has been supported by the European Communities under the contract of Association EURATOM/Hellenic Republic. The views and opinions expressed herein do not necessarily reflect those of the European Commission.

[1]F. Sharipov and V. Seleznev, J. Phys. Chem. Ref. Data **27**, 657 (1998).
[2]M. Hasegawa and Y. Sone, J. Vac. Soc. Jpn. **31**, 416 (1988).
[3]K. Aoki, "Numerical analysis of rarefied gas flows by finite-difference method," in *Rarefied Gas Dynamics*, edited by E. P. Muntz, D. P. Weaver, and D. H. Campbell (AIAA, Washington DC, 1989), Vol. 118, pp. 297.
[4]F. Sharipov, J. Vac. Sci. Technol. A **17**, 3062 (1999).
[5]I. Graur and F. Sharipov, Eur. J. Mech. B/Fluids **27**, 335 (2008).
[6]G. Breyiannis, S. Varoutis, and D. Valougeorgis, Eur. J. Mech. B/Fluids **27**, 609 (2008).
[7]S. Naris and D. Valougeorgis, Eur. J. Mech, B/Fluids **27**, 810 (2008).
[8]F. Sharipov and V. Seleznev, J. Vac. Sci. Technol. A **12**, 2933 (1994).
[9]S. Varoutis, S. Naris, V. Hauer, C. Day, and D. Valougeorgis, J. Vac. Sci. Technol. A **27**, 89 (2009).
[10]L. Szalmas, J. Pitakarnnop, S. Geoffroy, S. Colin, and D. Valougeorgis, Microfluid Nanofluid **9**, 1103 (2010).
[11]A. J. Osiadacz, Int. J. Syst. Sci. **19**, 2395 (1988).
[12]G. P. Greyvenstein and D. P. Laurie, Int. J. Numer. Meth. Eng. **37**, 3685 (1994).
[13]M. C. Potter and D. C. Wiggert, *Mechanics of Fluids*, 2nd ed. (Prentice Hall, New York, 1997).
[14]S. Dushman and J. M. Lafferty, *Scientific Foundations of Vacuum Technique*, 2nd ed. (Wiley, New York, 1962).
[15]S. Ohta, N. Yoshimura, and H. Hirano, J. Vac. Sci. Technol. A **1**, 84 (1983).
[16]V. Hauer and C. Day, Fusion Eng. Des. **84**, 903 (2009).
[17]F. Sharipov, J. Vac. Sci. Technol. A **14**, 2627 (1996).
[18]K. Jousten, *Handbook of Vacuum Technology* (Wiley, New York, 2008).